YMTHE, Volume *26*

Supplemental Information

Optimized Cholesterol-siRNA Chemistry Improves Productive Loading onto Extracellular Vesicles

Reka Agnes Haraszti, Rachael Miller, Marie-Cecile Didiot, Annabelle Biscans, Julia F. Alterman, Matthew R. Hassler, Loic Roux, Dimas Echeverria, Ellen Sapp, Marian DiFiglia, Neil Aronin, and Anastasia Khvorova

Optimized cholesterol-siRNA chemistry improves productive loading onto extracellular vesicles

Reka Agnes Haraszti[1,2], Rachael Miller[1,3], Marie-Cecile Didiot[1,2], Annabelle Biscans[1,2], Julia F Alterman[1,2], Matthew R Hassler[1,2], Loic Roux[1,2], Dimas Echeverria[1,2], Ellen Sapp[4], Marian DiFiglia[4], Neil Aronin[1,3]*, Anastasia Khvorova[1,2]*

[1]RNA Therapeutics Institute, University of Massachusetts Medical School, Worcester, MA, USA

[2]Program in Molecular Medicine, University of Massachusetts Medical School, Worcester, MA, USA

[3]Department of Medicine, University of Massachusetts Medical School, Worcester, MA, USA

[4]Mass General Institute for Neurodegenerative Disease, Boston, MA, USA

Correspondence should be addressed to:

Anastasia Khvorova (anastasia.khvorova@umassmed.edu; 774-455-3638 / 508-856-6696 (fax)) and Neil Aronin (neil.aronin@umassmed.edu; 508-856-6559 / 508-856-6696 (fax)), University of Massachusetts Medical School, 368 Plantation Street, Worcester, MA, 01605

Keywords: Extracellular vesicles; siRNA; oligonucleotides; nanovesicles; chemical modification; RNA therapy

Supplementary Information

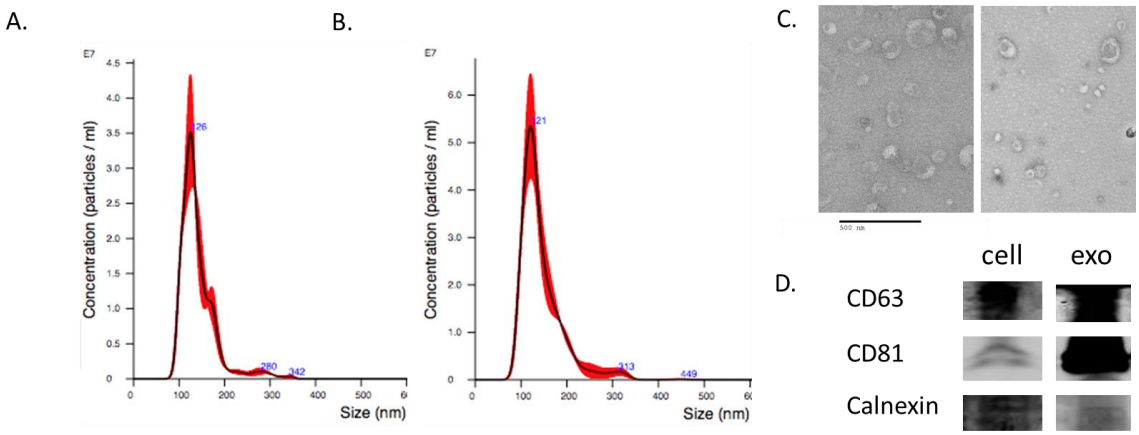

Supplementary Figure 1. Characterization of liposomes and umbilical cord, Wharton-s jelly derived extracellular vesicles A. Nanoparticle Tracking Analysis shows homogenous extracellular vesicle size distribution with mean diameter 141± 40 nm, n=3 **B.** Nanoparticle Tracking Analysis of neutral liposomes, mean diameter 144 ± 47 nm, n=3 **C.** Transmission Electron Microscopy image of unloaded (left) and loaded (right) extracellular vesicles, size bar shows 500 nm. **D.** Western blot of positive and negative extracellular vesicle marker proteins.

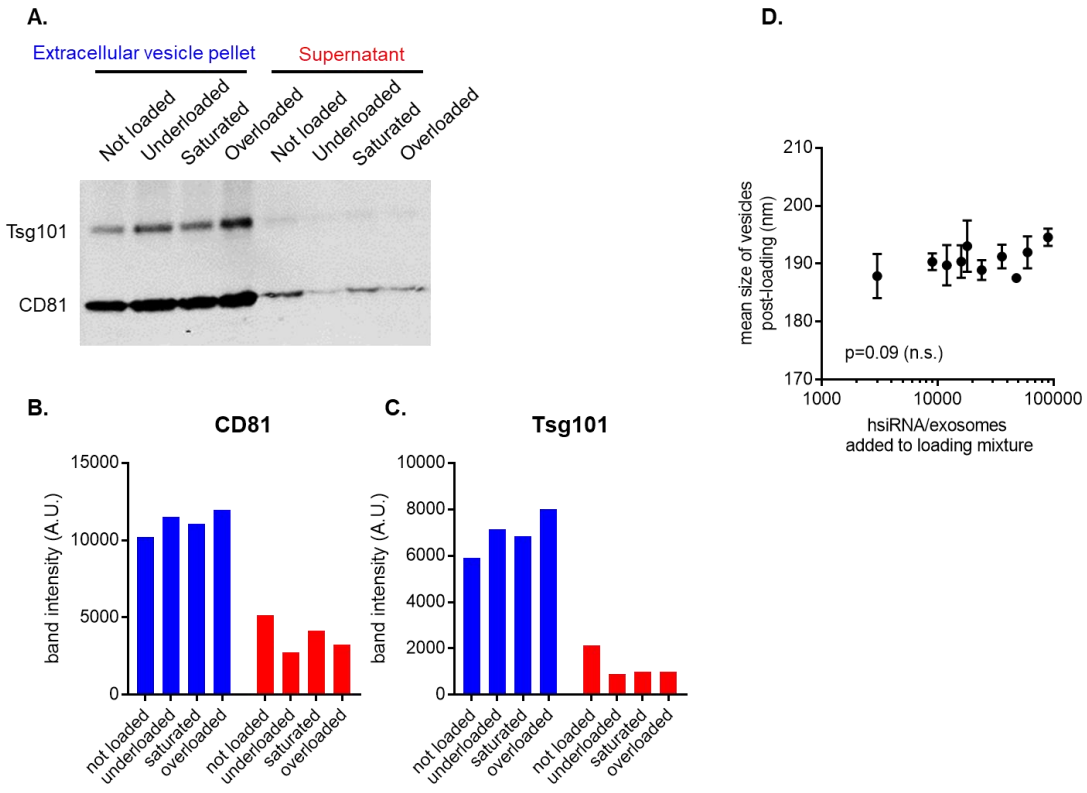

Supplementary Figure 2. Characterization of loaded extracellular vesicles A. Western blot of unloaded, underloaded, saturated and overloaded extracellular vesicles (0, 3000, 12 000 and 90 000 RNA molecules per vesicle mixed in; 0, 1900, 3700 and 14300 RNA molecules per vesicle loaded). After incubation at 37°C for 1 hour, extracellular vesicle-hsiRNA mixture was centrifuged at 100,000 g for 1 hour to pellet loaded extracellular vesicles (blue) and remove non-loaded siRNA (red). SDS-PAGE was conducted after lysis in RIPA. **B.** CD81 signal was quantified using ImageJ Gel Analysis tool. **C.** Tsg101 signal was quantified using ImageJ Gel Analysis tool. **D.** Size (average diameter of particles in nm) of loaded extracellular vesicles measured *via* Nanoparticle Tracking Analysis. n=3, mean ± SD

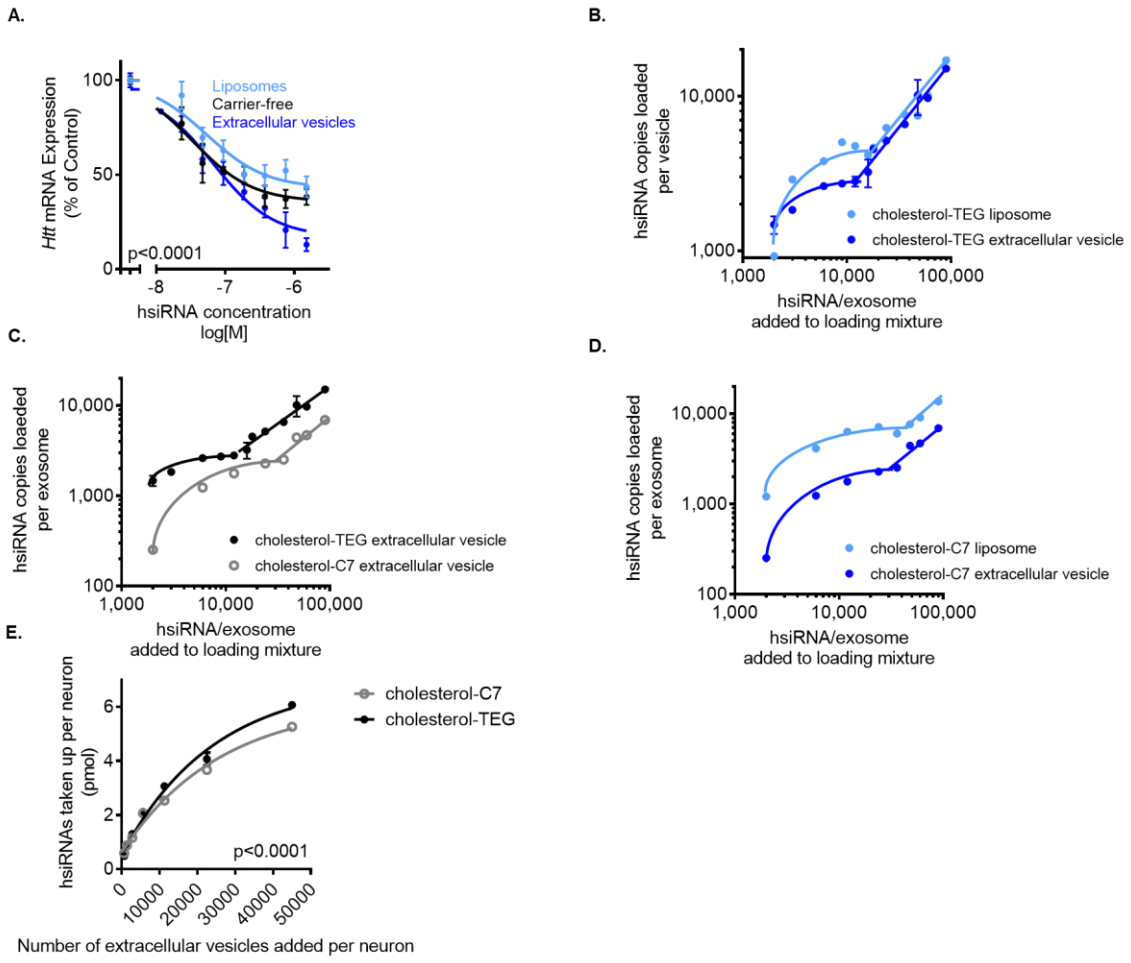

Supplementary Figure 3. Comparison of loaded extracellular vesicles *versus* loaded liposomes A. Silencing activity of hsiRNA loaded onto either extracellular vesicles (dark blue) or liposomes (light blue) or delivered carrier-free (black) to primary neurons. n=3, mean ± SEM **B-D.** Cholesterol-hsiRNA was loaded onto extracellular vesicles at different hsiRNA-to-extracellular vesicles ratios. The loading curve shows and initial saturation phase followed by a secondary linear phase. **E.** Guide strand accumulation of cholesterol-C7-hsiRNA and cholesterol-TEG-hsiRNA in neurons following delivery *via* extracellular vesicles. n=3, mean ± SEM, two-way ANOVA. Guide strand accumulation measured by PNA hybridization assay.

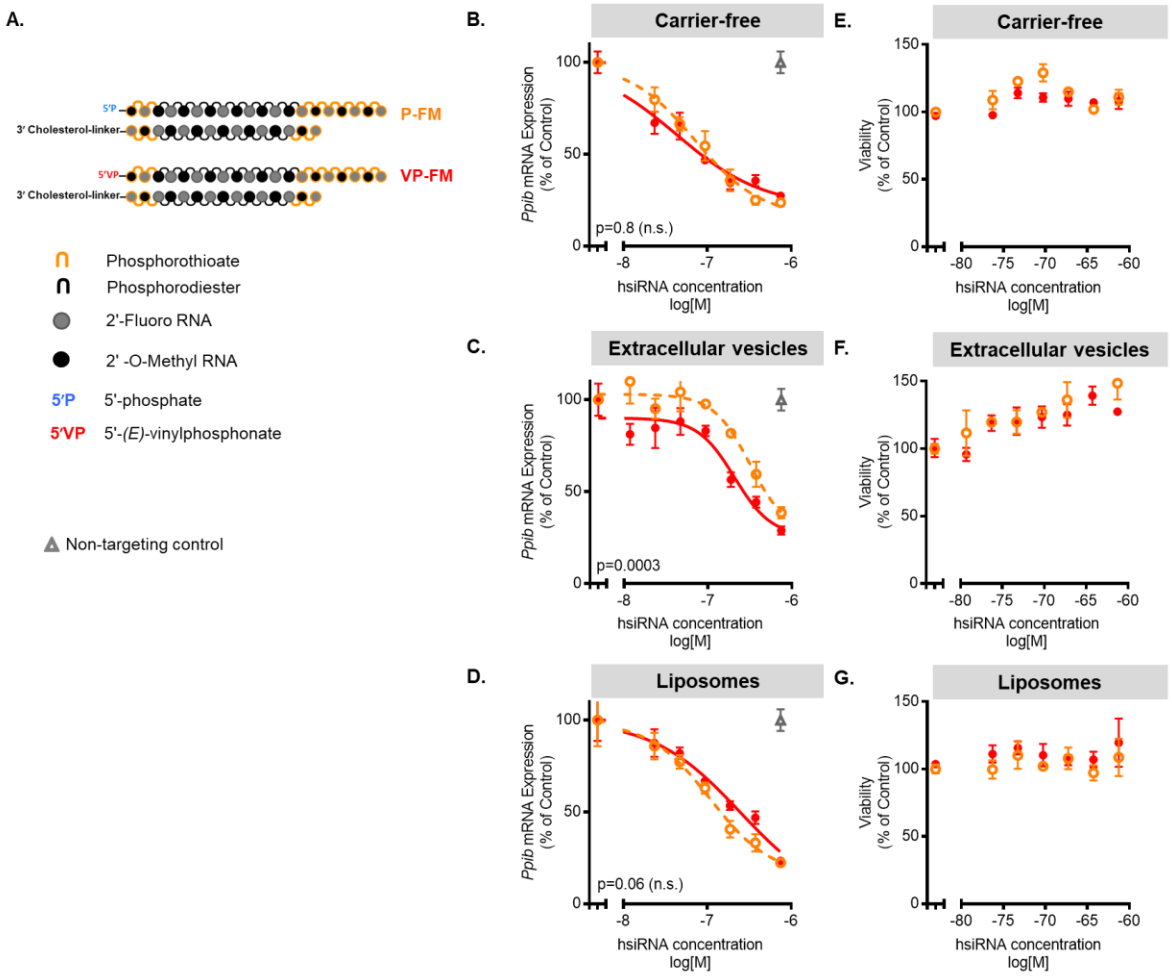

Supplementary Figure 4. Stabilization of 5′-phosphate is not toxic in and beneficial for EV-mediated delivery of siRNAs. A. Scheme of chemically modified hsiRNAs. P-FM fully modified backbone with 5′-phosphate on guide strand, VP-FM fully modified backbone with 5′-*(E)*-vinylphosphonate on guide strand. n=3, mean ± SEM **B-D.** HeLa cells were incubated for three days with cholesterol-hsiRNA variants with different 5′ end modifications either alone (carrier-free), or loaded onto extracellular vesicles or liposomes, target *Ppib* mRNA silencing was measured, and silencing potency calculated (IC50). n=3 Pairwise comparison of curves was conducted using two-way ANOVA. Significance is depicted in grey. **E-G.** Primary murine cortical neurons were incubated for one week with cholesterol-hsiRNA variants with different 5′ end modifications either alone (carrier-free),

or loaded onto extracellular vesicles or liposomes, targeting *Hunntingtin.* To measure cell viability, Alamar Blue® was added an incubated at 37℃ for 12 hours, and fluorescence measured at 570 nm excitation, 585 nm emission. Signal is normalized to non-treated cells samples. n=3, mean ± SD

Gene Targeted	Compound Name	Figure applicable	Strand	Sequence 5'-3'	Conjugate 5'	Conjugate 3'
Huntingtin	P-PM	Fig.3.	passenger	mC.mA.G.mU.A.A.A.G.A.G.A.mU.mU#mA#mA	Cy3	Cholesterol-TEG
			guide	PmU.fU.A.A.fU.fC.fU.fC.fU.fU.fU.A.fC.fU#G#A#fU#A#fU#A		
Huntingtin	VP-PM	Fig.3.	passenger	mC.mA.G.mU.A.A.A.G.A.G.A.mU.mU#mA#mA	Cy3	Cholesterol-TEG
			guide	VPmU.fU.A.A.fU.fC.fU.fC.fU.fU.fU.A.fC.fU#G#A#fU#A#fU#A		
Huntingtin	cholesterol-TEG hsiRNA P-FM	Fig.1-3.	passenger	fC#mA#fG.mU.fA.mA.fA.mG.fA.mG.fA.mU.fU#mA#fA	Cy3	Cholesterol-TEG
			guide	PmU#fU#mA.fA.mU.fC.mU.fC.mU.fU.mU.fA.mC#fU#mG#fA#mU#fA#mU#fA		
Huntingtin	VP-FM Endonuclase stable	Fig.3-4.	passenger	fC#mA#fG.mU.fA.mA.fA.mG.fA.mG.fA.mU.fU#mA#fA	Cy3	Cholesterol-TEG
			guide	VPmU#fU#mA.fA.mU.fC.mU.fC.mU.fU.mU.fA.mC#fU#mG#fA#mU#fA#mU#fA		
Huntingtin	cholesterol-C7	Fig.1.	passenger	fC#mA#fG.mU.fA.mA.fA.mG.fA.mG.fA.mU.fU#mA#fA	Cy3	Cholesterol-C7
			guide	PmU#fU#mA.fA.mU.fC.mU.fC.mU.fU.mU.fA.mC#fU#mG#fA#mU#fA#mU#fA		
Huntingtin	moderately endonuclease sensitive (DNA)	Fig.4.	passenger	fC#mA#fG.mU.A.mA.fA.mG.fA.mG.fA.mU.fU#mA#fA.dT.dT		Cholesterol-TEG
			guide	VPmU#fU#mA.fA.mU.fC.mU.fC.mU.fU.mU.fA.mC#fU#mG#fA#mU#fA#mU#fA		
Huntingtin	highly endonuclease sensitive (RNA)	Fig.4.	passenger	fC#mA#fG.mU.A.mA.fA.mG.fA.mG.fA.mU.fU#mA#fA.rU.rU		Cholesterol-TEG
			guide	VPmU#fU#mA.fA.mU.fC.mU.fC.mU.fU.mU.fA.mC#fU#mG#fA#mU#fA#mU#fA		
PPIB	P-FM	Supp.Fig.4.	passenger	fC#mA#fA.mA.fU.mU.fC.mC.fA.mU.fC.mG.fU#mG#fA	Cy3	Cholesterol-TEG
			guide	PmU#fC#mA.fC.mG.fA.mU.fG.mG.fA.mA.fU.mU#fU#mG#fC#mU#fG#mU#fU		
PPIB	VP-FM	Supp.Fig.4.	passenger	fC#mA#fA.mA.fU.mU.fC.mC.fA.mU.fC.mG.fU#mG#fA	Cy3	Cholesterol-TEG
			guide	vPmU#fC#mA.fC.mG.fA.mU.fG.mG.fA.mA.fU.mU#fU#mG#fC#mU#fG#mU#fU		

Supplementary Table 1. Table describing hsiRNA sequences used in this study. m = 2′ -O-methyl; f = 2′ -fluoro; # = phosphorothioate; P = phosphate; VP = 5′ -(E)-vinylphosphonate; TEG = triethyl glycol; C7 = 2-aminobutyl-1-3-propanediol

P49184	DNSL1	HUMAN Deoxyribonuclease-1-like 1 OS=Homo sapiens GN=DNASE1L1 PE=1 SV=1	34 kDa
Q7KZF4	SND1	HUMAN Staphylococcal nuclease domain-containing protein 1 OS=Homo sapiens GN=SND1 PE=1 SV=1	102 kDa
O94919	ENDD1	HUMAN Endonuclease domain-containing 1 protein OS=Homo sapiens GN=ENDOD1 PE=1 SV=2	55 kDa
P13489	RINI	HUMAN Ribonuclease inhibitor OS=Homo sapiens GN=RNH1 PE=1 SV=2	50 kDa
P21589	5NTD	HUMAN 5'-nucleotidase OS=Homo sapiens GN=NT5E PE=1 SV=1	63 kDa
P22413	ENPP1	HUMAN Ectonucleotide pyrophosphatase/phosphodiesterase family member 1 OS=Homo sapiens GN=ENPP1 PE=1 SV=2	105 kDa
P09543	CN37	HUMAN Isoform CNPI of 2',3'-cyclic-nucleotide 3'-phosphodiesterase OS=Homo sapiens GN=CNP	45 kDa

Supplementary Table 2. Nucleases detected in extracellular vesicles